COMMUNICATIONS IN NUMERICAL METHODS IN ENGINEERING
Commun. Numer. Meth. Engng 2002; **18**:1–10 *Prepared using* cnmauth.cls *[Version: 2000/03/22 v1.0]*

Dual analysis by a meshless method

Marc Duflot[1,*] and Hung Nguyen-Dang[1]

[1] *Fracture mechanics department, University of Liège, Chemin des chevreuils 1, 4000 Liège, Belgium*

SUMMARY

A meshless method to solve elastostatics problems based on an equilibrium model is presented. This means that the equilibrium and constitutive equations are satisfied a priori and that the approximation only concerns the compatibility equations. The application of this method together with the classical displacement meshless method leads to upper and lower bounds on the energy. The difference between these bounds gives a global error estimation on the solution. Copyright © 2002 John Wiley & Sons, Ltd.

KEY WORDS: meshless method, dual analysis

1. INTRODUCTION

Dual analysis for the resolution of solid mechanics problems consists in using two conjugate models. One is the displacement model, satisfying compatibility and violating equilibrium, and the other is the equilibrium (or stress based) model, satisfying equilibrium and violating compatibility. The purpose of the dual analysis is to obtain upper and lower bounds on characteristic values, such as the energy or a load factor. An error estimation on the approximate solution is obtained by comparing the bounds yielded by both models. This estimation is essential to ensure the reliability of the computation. The dual analysis was first introduced by Fraeijs de Veubeke [1, 2] in the framework of the finite element method. The analysis in this paper is based on the more recent and more general formulation of Debongnie, Zhong and Beckers [3].

The purpose of this paper is to realize a dual analysis with two meshless methods. The displacement meshless method is now well-known and has been widely used during the last decade, see for example Belytschko, Lu and Gu [4]. The equilibrium meshless method is developed in this paper for the first time. The difficult point in this new approach is to satisfy the equilibrium at each point in the domain. To that end, the stresses are expressed by means of an Airy stress function. It is worth mentioning a few papers dealing with equilibrium finite

*Correspondence to: Marc Duflot, Fracture mechanics department, University of Liège, Chemin des chevreuils 1, 4000 Liège, Belgium. E-mail: m.duflot@ulg.ac.be

Contract/grant sponsor: Belgian National Fund for Scientific Research (F.N.R.S.)

element methods based on an Airy stress function: Fraeijs de Veubeke and Zienkiewicz [5], Gallagher and Dhalla [6], Vallabhan and Azene [7] and Sarigul and Gallagher [8].

The outline of this paper goes as follows. In section 2, the main results of the dual analysis for upper and lower bounds on the total complementary energy in elasticity are presented. In section 3, we recall the displacement meshless method and we develop the equilibrium meshless method. Two numerical examples illustrate the proposed dual analysis in section 4. Finally, in section 5, we discuss the advantages and drawbacks of the equilibrium model over the displacement model, draw some conclusions and open some perspectives.

2. DUAL ANALYSIS

In this section, we present the global error estimation method in elastostatics by dual analysis; we refer to [3] for the proofs and details. Let us consider a linear elastic solid that occupies a domain Ω bounded by Γ subject to the body force $\overline{\mathbf{b}}$ in Ω, to the surface tractions $\overline{\mathbf{t}}$ on Γ_t and with prescribed displacements $\overline{\mathbf{u}}$ on Γ_u (with $\Gamma_t \bigcap \Gamma_u = \emptyset$ and $\Gamma_t \bigcup \Gamma_u = \Gamma$). The relations between the displacement field $\mathbf{u}$, the strain field $\boldsymbol{\varepsilon}$ and the stress field $\boldsymbol{\sigma}$ are

1. the compatibility relations
$$\boldsymbol{\varepsilon} = \nabla_s \mathbf{u}^{\mathrm{T}} \text{ in } \Omega \tag{1}$$
$$\mathbf{u} = \overline{\mathbf{u}} \text{ on } \Gamma_u \tag{2}$$
where $\nabla_s \mathbf{u}^{\mathrm{T}}$ is the symmetric part of $\nabla \mathbf{u}^{\mathrm{T}}$,
2. the constitutive relations
$$\boldsymbol{\sigma} = \mathbf{D} : \boldsymbol{\varepsilon} \text{ in } \Omega \tag{3}$$
where $\mathbf{D}$ is the Hooke tensor and
3. the equilibrium equations
$$\nabla^{\mathrm{T}} \boldsymbol{\sigma} + \overline{\mathbf{b}} = 0 \text{ in } \Omega \tag{4}$$
$$\boldsymbol{\sigma}\mathbf{n} = \overline{\mathbf{t}} \text{ on } \Gamma_t \tag{5}$$
where $\mathbf{n}$ is the outer normal.

The total energy is defined as

$$E_T(\mathbf{u}) = E_U(\mathbf{u}) + E_P(\mathbf{u}) \tag{6}$$

where

$$E_U(\mathbf{u}) = \frac{1}{2} \int_\Omega \boldsymbol{\varepsilon}(\mathbf{u}) : \mathbf{D} : \boldsymbol{\varepsilon}(\mathbf{u}) \, d\Omega \tag{7}$$

is the strain energy and

$$E_P(\mathbf{u}) = -\int_\Omega \overline{\mathbf{b}}^{\mathrm{T}} \cdot \mathbf{u} \, d\Omega - \int_{\Gamma_t} \overline{\mathbf{t}}^{\mathrm{T}} \cdot \mathbf{u} \, d\Gamma \tag{8}$$

is the potential energy of the prescribed loads. The total complementary energy is defined as

$$E_C(\boldsymbol{\sigma}) = E_V(\boldsymbol{\sigma}) + E_Q(\boldsymbol{\sigma}) \tag{9}$$

where

$$E_V(\boldsymbol{\sigma}) = \frac{1}{2}\int_\Omega \boldsymbol{\sigma} : \mathbf{D}^{-1} : \boldsymbol{\sigma}\, d\Omega \tag{10}$$

is the complementary strain energy and

$$E_Q(\boldsymbol{\sigma}) = -\int_{\Gamma_u} \overline{\mathbf{u}}^{\mathrm{T}} \boldsymbol{\sigma}\mathbf{n}\, d\Gamma \tag{11}$$

is the potential energy of the prescribed displacements. It can easily be shown that the exact solution of equations (1) to (5) verifies the following property:

$$-E_T(\mathbf{u}_{\text{exact}}) = E_C(\boldsymbol{\sigma}_{\text{exact}}) \tag{12}$$

We use the notation E_{exact} for the exact total complementary energy $E_C(\boldsymbol{\sigma}_{\text{exact}})$ in the following. To approximate the exact solution, one can either use a displacement model, which is the common choice, or an equilibrium model.

Displacement model An admissible displacement field, also called a kinematically admissible field, a priori satisfies the compatibility equations (1) and (2) and the constitutive equations (3). It can be shown that, among all admissible displacement fields, the exact field minimizes the total energy. In other words, for each $\mathbf{u}_h$ kinematically admissible, the following inequality holds:

$$E_T(\mathbf{u}_h) \geq E_T(\mathbf{u}_{\text{exact}}) \tag{13}$$

Equilibrium model An admissible stress field, also called a statically admissible field, a priori satisfies the constitutive equations (3) and the equilibrium equations (4) and (5). It can be shown that, among all admissible stress fields, the exact field minimizes the total complementary energy. In other words, for each $\boldsymbol{\sigma}_h$ statically admissible, the following inequality holds:

$$E_C(\boldsymbol{\sigma}_h) \geq E_C(\boldsymbol{\sigma}_{\text{exact}}) \tag{14}$$

Fundamental result Equations (12), (13) and (14) lead to the following lower and upper bounds on the exact total complementary energy:

$$-E_T(\mathbf{u}_h) \leq E_{\text{exact}} \leq E_C(\boldsymbol{\sigma}_h) \tag{15}$$

So, the half-sum of the total energy of a kinematically admissible field and of the total complementary energy of a statically admissible field gives an estimation of the global error yielded by both of these approximations. In this paper, both approximations are obtained by Rayleigh-Ritz processes, based on meshless shape functions.

3. MESHLESS METHOD

Consider a set of N nodes scattered in a domain Ω and let $\mathbf{x}_i$ be the coordinates of node i. The moving least squares approximation $\mathbf{f}_h(\mathbf{x})$ of a (multi-dimensional) field $\mathbf{f}(\mathbf{x})$ in Ω is (see [4] for details):

$$\mathbf{f}_h(\mathbf{x}) = \sum_{i=1}^{N} \phi_i(\mathbf{x})\, \mathbf{f}_i \tag{16}$$

where $\mathbf{f}_i$ is the value of the field $\mathbf{f}$ at $\mathbf{x}_i$ and ϕ_i is the shape function of node i, given by

$$\phi_i(\mathbf{x}) = \mathbf{c}^{\mathrm{T}}(\mathbf{x})\,\mathbf{p}(\mathbf{x}_i)\,w_i(\mathbf{x}) \tag{17}$$

where $\mathbf{p}(\mathbf{x})$ is a set of basis functions (usually the set of monomials up to a given order), $w_i(\mathbf{x})$ is a weight function associated with node i and

$$\mathbf{c}(\mathbf{x}) = \mathbf{A}^{-1}(\mathbf{x})\,\mathbf{p}(\mathbf{x}) \tag{18}$$

with

$$\mathbf{A}(\mathbf{x}) = \sum_{i=1}^{N} w_i(\mathbf{x})\,\mathbf{p}(\mathbf{x}_i)\,\mathbf{p}^{\mathrm{T}}(\mathbf{x}_i) \tag{19}$$

A small domain Ω_i containing $\mathbf{x}_i$ is associated with node i such that $w_i(\mathbf{x})$ and, as a result, $\phi_i(\mathbf{x})$ equal zero outside Ω_i. This choice is made in order to provide the approximation with a local character and to restrict the sums in equations (16) and (19) to a few terms. In this work, we use the isotropic quartic spline function:

$$w_i(\mathbf{x}) = \begin{cases} 1 - 6s^2 + 8s^3 - 3s^4 & \text{if } s \leq 1 \\ 0 & \text{if } s > 1 \end{cases} \quad \text{with } s = \frac{\|\mathbf{x} - \mathbf{x}_i\|}{r_i} \tag{20}$$

where r_i is the support radius of node i.

We will need the expression of the first- and second-order partial derivatives of this shape function with respect to the coordinate x_k for $k = 1, \ldots, n_{\mathrm{dim}}$ (n_{dim} is the number of dimensions). They are given by:

$$\phi_{i,k}(\mathbf{x}) = \mathbf{c}_{,k}^{\mathrm{T}}(\mathbf{x})\,\mathbf{p}(\mathbf{x}_i)\,w_i(\mathbf{x}) + \mathbf{c}^{\mathrm{T}}(\mathbf{x})\,\mathbf{p}(\mathbf{x}_i)\,w_{i,k}(\mathbf{x}) \tag{21}$$

$$\begin{aligned} \phi_{i,kl}(\mathbf{x}) &= \mathbf{c}_{,kl}^{\mathrm{T}}(\mathbf{x})\,\mathbf{p}(\mathbf{x}_i)\,w_i(\mathbf{x}) + \mathbf{c}_{,k}^{\mathrm{T}}(\mathbf{x})\,\mathbf{p}(\mathbf{x}_i)\,w_{i,l}(\mathbf{x}) \\ &+ \mathbf{c}_{,l}^{\mathrm{T}}(\mathbf{x})\,\mathbf{p}(\mathbf{x}_i)\,w_{i,k}(\mathbf{x}) + \mathbf{c}^{\mathrm{T}}(\mathbf{x})\,\mathbf{p}(\mathbf{x}_i)\,w_{i,kl}(\mathbf{x}) \end{aligned} \tag{22}$$

with

$$\mathbf{c}_{,k}(\mathbf{x}) = \mathbf{A}^{-1}(\mathbf{x})\left[\mathbf{p}_{,k}(\mathbf{x}) - \mathbf{A}_{,k}(\mathbf{x})\,\mathbf{c}(\mathbf{x})\right] \tag{23}$$

$$\mathbf{c}_{,kl}(\mathbf{x}) = \mathbf{A}^{-1}(\mathbf{x})\left[\mathbf{p}_{,kl}(\mathbf{x}) - \mathbf{A}_{,k}(\mathbf{x})\,\mathbf{c}_{,l}(\mathbf{x}) - \mathbf{A}_{,l}(\mathbf{x})\,\mathbf{c}_{,k}(\mathbf{x}) - \mathbf{A}_{,kl}(\mathbf{x})\,\mathbf{c}(\mathbf{x})\right] \tag{24}$$

and

$$\mathbf{A}_{,k}(\mathbf{x}) = \sum_{i=1}^{N} w_{i,k}(\mathbf{x})\,\mathbf{p}(\mathbf{x}_i)\,\mathbf{p}^{\mathrm{T}}(\mathbf{x}_i) \tag{25}$$

$$\mathbf{A}_{,kl}(\mathbf{x}) = \sum_{i=1}^{N} w_{i,kl}(\mathbf{x})\,\mathbf{p}(\mathbf{x}_i)\,\mathbf{p}^{\mathrm{T}}(\mathbf{x}_i) \tag{26}$$

Meshless displacement model For the sake of completeness, we recall the well-known displacement model. The displacement field $\mathbf{u}(\mathbf{x})$ is approximated in the moving least-squares sense by $\mathbf{u}_h(\mathbf{x})$ given by

$$\mathbf{u}_h(\mathbf{x}) = \sum_{i=1}^{N} \phi_i(\mathbf{x})\, \mathbf{u}_i \tag{27}$$

where the $\phi_i(\mathbf{x})$ are the meshless shape functions (17) and the degrees of freedom $\mathbf{u}_i$ are arranged in a vector $\mathbf{q}$ that is determined by minimizing the total energy (6). This leads to a linear system

$$\mathbf{K}\mathbf{q} = \mathbf{g} \tag{28}$$

with $\mathbf{K}$, the stiffness matrix, consisting in submatrices $\mathbf{K}_{ij}$ of size $n_{\text{dim}} \times n_{\text{dim}}$ and $\mathbf{g}$ consisting in subvectors $\mathbf{g}_i$ of size n_{dim} given by

$$\mathbf{K}_{ij} = \int_{\Omega} \mathbf{B}_i^{\mathrm{T}} \mathbf{D} \mathbf{B}_j \, d\Omega \tag{29}$$

$$\mathbf{g}_i = \int_{\Gamma_t} \phi_i \overline{\mathbf{t}} \, d\Gamma + \int_{\Omega} \phi_i \overline{\mathbf{b}} \, d\Gamma \tag{30}$$

For two-dimensional problems, we have

$$\mathbf{B}_i = \begin{pmatrix} \phi_{i,x} & 0 \\ 0 & \phi_{i,y} \\ \phi_{i,y} & \phi_{i,x} \end{pmatrix} \tag{31}$$

and

$$\mathbf{D} = \frac{E}{1-\nu^2} \begin{pmatrix} 1 & \nu & 0 \\ \nu & 1 & 0 \\ 0 & 0 & \frac{1-\nu}{2} \end{pmatrix} \tag{32}$$

for an isotropic solid in plane stress where E and ν are respectively the Young modulus and Poisson ratio. We use a linear basis ($\mathbf{p}(\mathbf{x}) = [1\, x\, y]^{\mathrm{T}}$ in 2D) to be able to exactly represent a constant stress field. We also choose the support radius of the shape functions to be equal to $1.4\, h$, where h is the characteristic nodal spacing. The essential boundary conditions (2) are enforced with the help of Lagrangian multipliers in the same manner as in [4]: At several points on Γ_u, a degree of freedom is added to the linear system to relax the constraint

$$\sum_{i=1}^{N} \phi_i(\mathbf{x})\, \mathbf{u}_i = \overline{\mathbf{u}} \tag{33}$$

Meshless equilibrium model This model is restricted to problems with a body force deriving from a potential:

$$\overline{\mathbf{b}} = -\nabla \overline{V} \tag{34}$$

The difficulty in the equilibrium model is to satisfy equation (4) in the whole domain. To that end, we decide to express the stress field as

$$\boldsymbol{\sigma} = \left(\triangle \psi + \overline{V}\right) \mathbf{I} - \nabla \nabla^{\mathrm{T}} \psi \tag{35}$$

where $\triangle$ is the Laplacian $\nabla^{\mathrm{T}} \cdot \nabla$ and $\mathbf{I}$ is the identity matrix. ψ is called the Airy stress function, see for example [9]. For two-dimensional problems, this expression becomes

$$\begin{bmatrix} \sigma_x \\ \sigma_y \\ \tau_{xy} \end{bmatrix} = \begin{bmatrix} \psi_{,yy} + \overline{V} \\ \psi_{,xx} + \overline{V} \\ -\psi_{,xy} \end{bmatrix} \tag{36}$$

The Airy stress function $\psi(\mathbf{x})$ is approximated in the moving least-squares sense by $\psi_h(\mathbf{x})$ given by

$$\psi_h(\mathbf{x}) = \sum_{i=1}^{N} \phi_i(\mathbf{x})\, \psi_i \tag{37}$$

where the $\phi_i(\mathbf{x})$ are the meshless shape functions (17). Since we chose an isotropic quartic spline function, which possesses continuous second order derivatives, as the weight functions, $\psi_h(\mathbf{x})$ also possesses continuous second order derivatives and $\boldsymbol{\sigma}_h(\mathbf{x})$ is continuous. The degrees of freedom ψ_i are arranged in a vector $\mathbf{a}$ that is determined by minimizing the total complementary energy (9). This leads to a linear system

$$\mathbf{F}\mathbf{a} = \mathbf{d} \tag{38}$$

where the elements of the flexibility matrix $\mathbf{F}$ and of the vector $\mathbf{d}$ are given by

$$F_{ij} = \int_{\Omega} \mathbf{C}_i^{\mathrm{T}} \mathbf{D}^{-1} \mathbf{C}_j \, d\Omega \tag{39}$$

$$d_i = \int_{\Gamma_u} \mathbf{C}_i^{\mathrm{T}} \mathbf{N} \overline{\mathbf{u}} \, d\Gamma - \int_{\Omega} \overline{V} \boldsymbol{\delta}^{\mathrm{T}} \mathbf{D}^{-1} \mathbf{C}_i \, d\Omega \tag{40}$$

For two-dimensional problems, we have

$$\mathbf{C}_i = \begin{pmatrix} \phi_{i,yy} \\ \phi_{i,xx} \\ -\phi_{i,xy} \end{pmatrix} \tag{41}$$

$$\mathbf{N} = \begin{pmatrix} n_x & 0 \\ 0 & n_y \\ n_y & n_x \end{pmatrix} \tag{42}$$

$$\boldsymbol{\delta} = \begin{pmatrix} 1 \\ 1 \\ 0 \end{pmatrix} \tag{43}$$

We use a quadratic basis ($\mathbf{p}(\mathbf{x}) = \begin{bmatrix} 1\, x\, y\, x^2\, y^2\, xy \end{bmatrix}^{\mathrm{T}}$ in 2D) to be able to exactly represent a constant stress field. We choose the support radius of the shape functions to be equal to $2.8\, h$. The essential boundary conditions (5) are enforced with the help of Lagrangian multipliers: At several points on Γ_t, a degree of freedom is added to the linear system to relax the constraint

$$\left[\left(\sum_{i=1}^{N} \triangle \phi_i(\mathbf{x})\ \psi_i + \overline{V} \right) \mathbf{I} - \sum_{i=1}^{N} \nabla \nabla^{\mathrm{T}} \phi_i(\mathbf{x})\ \psi_i \right] .\mathbf{n} = \overline{\mathbf{t}} \tag{44}$$

We choose the number of points where the boundary conditions are enforced to be equal to the number of nodes on Γ_t. This technique using Lagrangian multipliers is similar in principle to what is done in the displacement model, but it is more complicated because it uses the second derivatives of the shape functions. A drawback of the equilibrium model is that it needs more Lagrangian multipliers since, in practical problems such as the beam problem 4.1, Γ_t is longer than Γ_u.

4. NUMERICAL EXAMPLES

4.1. Clamped beam

We solve the problem of a clamped beam submitted to a parabolic shear force, as can be seen in figure (1), by displacement and equilibrium models. The numerical values are $E = 3.10^7$, $\nu = 0.3$ and the total force $P = 250$. There is no body force and plane stress conditions are assumed. The nodes of the meshless approximation are regularly spaced; the coarsest set of nodes is shown on figure 1. The results for various nodal spacings can be found in table I and figure 2. As predicted by the theory, the values $-E_T(\mathbf{u}_h)$ and $E_C(\boldsymbol{\sigma}_h)$ converge towards each other; $-E_T(\mathbf{u}_h)$ converges with increasing values and $E_C(\boldsymbol{\sigma}_h)$ converges with decreasing values. Moreover, these results are in close agreement with the result 0.0393955 of Zhong [10] obtained by a Richardson's extrapolation method based on finite element results. The difference between the energies for the finest set of nodes is about 0.2%.

4.2. Cracked plate

We solve the problem of the plate in stretching with an edge crack using twofold symmetry. The domain is a square with the exact mode I asymptotic displacement field enforced on three sides and no traction on the fourth side, which contains the crack, as can be seen in figure 3. This figure also shows the coarsest set of nodes. The numerical values are $E = 1$, $\nu = 0.3$ and the mode I stress intensity factor $K_I = 1$. There is no body force and plane stress conditions are assumed. The exact total complementary energy equals -0.417400. The results for various sets of regularly spaced nodes can be found in table II and figure 4; they are in good agreement with the exact value. As in the previous example, the convergence of the energies towards the exact value follows the theory. The difference between the energies for the finest set of nodes is about 2%. For a given number of nodes, the displacement model gives an energy closer to the exact result.

5. DISCUSSION AND CONCLUSIONS

In this paper, we presented a new meshless method to solve elastostatics problems based on a equilibrium model. The equilibrium equations and the constitutive equations are satisfied a priori and the approximation is realized on the compatibility equations. To satisfy the equilibrium equations at each point of the domain, we derive the stresses from an Airy stress function. This function is approximated by a linear combination of meshless shape functions. We note that the smoothness of the meshless shape functions is an essential property that permits to conceive this method. The drawback of this method when comparing with the

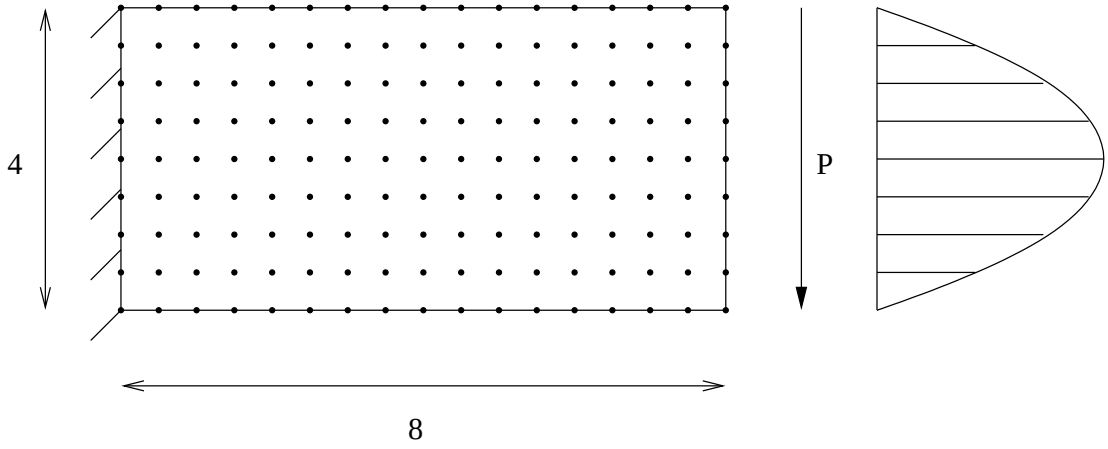

Figure 1. Clamped beam submitted to a parabolic shear force (17×9 nodes)

Number of nodes	Nodal spacing	Displacement model $-E_T$	Stress model E_C
$17 \times 9 = 153$	0.5	0.0391579	0.0405188
$33 \times 17 = 561$	0.25	0.0393393	0.0396398
$49 \times 25 = 1225$	0.166667	0.0393768	0.0395232
$65 \times 33 = 2145$	0.125	0.0393911	0.0394816

Table I. Results of the beam problem

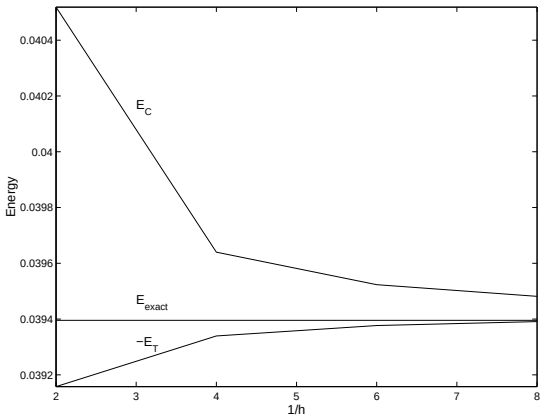

Figure 2. Convergence curves for the beam problem

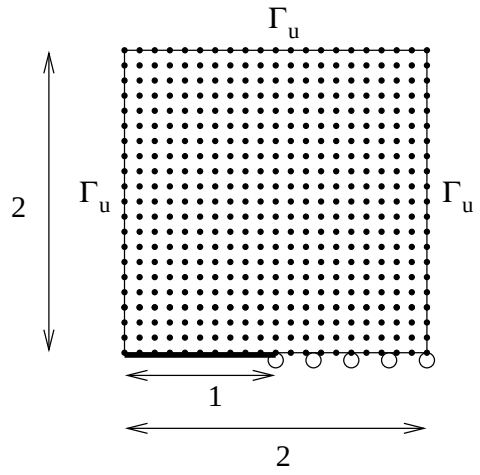

Figure 3. Cracked plate with prescribed displacement on three sides (21×21 nodes)

Number of nodes	Nodal spacing	Displacement model $-E_T$	Stress model E_C
$21 \times 21 = 441$	0.1	-0.426003	-0.394501
$41 \times 41 = 1681$	0.05	-0.421725	-0.405843
$61 \times 61 = 3721$	0.0333333	-0.420288	-0.409678
$81 \times 81 = 6561$	0.025	-0.419569	-0.411418

Table II. Results of the crack problem

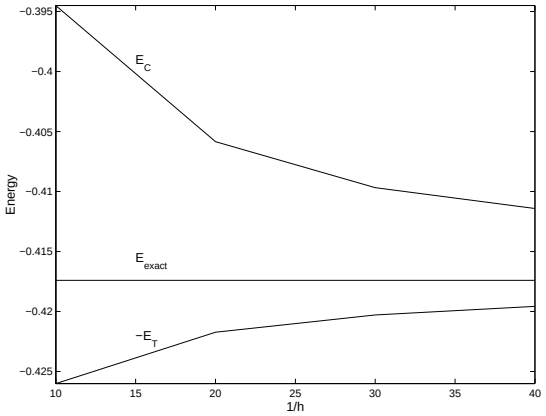

Figure 4. Convergence curves for the crack problem

traditional displacement model is that it requires the second order derivatives of the meshless shape functions, and mainly that a quadratic basis must be used. However, an advantage is that there is only one degree of freedom associated with each node while in the traditional method, the number of degrees of freedom for each node is equal to the number of space dimensions. The numerical tests show that, for a given number of nodes, the traditional method gives better results than the new method. Nevertheless, our aim was not to replace the displacement model with the equilibrium model but rather to obtain a global error estimator based upon the combination of both models. In this respect, the numerical examples show that the new method fulfills our objectives.

The method was illustrated in two-dimensional linear elasticity but it can be extended. Firstly, the method can be applied in nonlinear elasticity since it can be shown that the fundamental result (15) is also verified. Secondly, the method can be applied in three dimensions, where the reduction of the number of degrees of freedom between the new and the traditional methods is 3 instead of 2. The method in three dimensions is similar to what was done in this paper: Equation (35) is indeed still valid to obtain an equilibrated three-dimensional stress field and equation (37) is also an appropriate expression for the meshless approximation of the stress function. The next step will be to use the dual analysis on problems where the meshless method proved to be particularly efficient, such as fracture mechanics problems. Finally, we expect that the dual analysis will be a mean to control the refinement of the set of nodes to obtain a solution under a prescribed accuracy.

ACKNOWLEDGEMENTS

The support of the Belgian National Fund for Scientific Research (F.N.R.S.) to Marc Duflot is gratefully acknowledged.

REFERENCES

1. Fraeijs de Veubeke B. Upper and lower bounds in matrix structural analysis. In *AGARDograph 72: Matrix Methods of Structural Analysis*. Pergamon Press: London, 1963; 165–201.
2. Fraeijs de Veubeke B. Displacement and equilibrium models in the finite element method. In *Stress Analysis*, Zienkiewicz OC, Holister G (eds). John Wiley and Sons, 1965: chapter 9, 145–197. Reprinted in *International Journal for Numerical Methods in Engineering* 2001; **52**:287–342.
3. Debongnie JF, Zhong HG, Beckers P. Dual analysis with general boundary conditions. *Computer Methods in Applied Mechanics and Engineering* 1995; **122**:183–192.
4. Belytschko T, Lu YY, Gu L. Element-free Galerkin methods. *International Journal for Numerical Methods in Engineering* 1994; **37**:229–256.
5. Fraeijs de Veubeke B, Zienkiewicz OC. Strain-energy bounds in finite-element analysis by slab analogy. *Journal of Strain Analysis* 1967; **2**(4):265–271.
6. Gallagher RH, Dhalla AK. Direct flexibility finite element elastoplastic analysis. In *Proceedings of the First International Conference on Structural Mechanics in Reactor Technology*. Berlin, 1971; 443–462.
7. Vallabhan CVG, Azene M. A finite element model for plane elasticity problems using the complementary energy theorem. *International Journal for Numerical Methods in Engineering* 1982; **18**:291–309.
8. Sarigul N, Gallagher RH. Assumed stress function finite element method: Two-dimensional elasticity. *International Journal for Numerical Methods in Engineering* 1989; **28**:1577–1598.
9. Timoshenko SP, Goodier SN. *Theory of Elasticity*. McGraw-Hill: New York, 1987.
10. Zhong HG. *Estimateurs d'erreur a posteriori et adaptation de maillages dans la méthode des éléments finis*. PhD thesis, University of Liège, 1991.